Synthesis and Properties of Novel Low-Band-Gap Thienopyrazine-Based Poly(heteroarylenevinylene)s

Munazza Shahid,[†] Raja Shahid Ashraf,*[,†] Elisabeth Klemm,*[,†] and Steffi Sensfuss[‡]

Institut für Organische Chemie und Makromolekulare Chemie der Friedrich-Schiller-Universität Jena, Humboldtstrasse 10, D-07743 Jena, Germany, and Thüringisches Institut für Textil- und Kunststoff-Forschung Rudolstadt, Breitscheidstrasse 97, D-07407 Rudolstadt, Germany

Received June 2, 2006; Revised Manuscript Received August 10, 2006

ABSTRACT: Thieno[3,4-*b*]pyrazine-based poly(heteroarylenevinylene)s (PHAVs) (**P-1**−**P-6**) by Horner polycondensation and cyano-PHAVs (**P-7**−**P-9**) by Knoevenagel polycondensation have been synthesized in quantitative yields. The copolymers are characterized by NMR, IR, UV, GPC, and elemental analysis. High molecular weight ($\bar{M}_w$ up to 279 000 g/mol), thermostable, soluble, and film-forming materials were obtained. The absorption spectra of the polymers show two peaks located in the UV and visible region from ∼384 to 650 nm and are promising for the application in polymer solar cells. The absorption and emission in solution and in solid state of the polymers revealed that the polymers generate a π-stacked structure in the solid state, and the polymer molecules in the film were ordered. Thin films of the polymers **P-1**−**P-9** exhibit an optical band gap of ∼1.56−2.08 eV. Cyclic voltammograms display that the p-doping/dedoping and n-doping/dedoping processes of the polymers (**P-1**, **P-2, P-3, P-5**, and **P-6**) are reversible. The HOMO and LUMO levels of the polymers were determined from electrochemical measurements. From the absorption spectra of the polymers (**P-1**, **P-2**, and **P-8**) in chloroform/methanol mixtures, all the three polymers have revealed solvatochromic effects, which have been related to the formation of aggregates.

Introduction

In the past two decades, π-conjugated polymers have received considerable attention due to their excellent electronic and optoelectronic properties.[1] Presently, conjugated polymers are used for a variety of optoelectronic applications such as light-emitting diodes,[2,3] photovoltaic devices,[4,5] and field-effect transistors.[6,7]

Low-band-gap conjugated polymers are promising materials for the development of organic solar cells due to the improved harvest of the solar emission.[8] The synthetic principles for lowering the band gap have been reviewed.[9] A reduction of the band gap of conjugated polymers can be accomplished, among other ways, by minimizing the bond length alternation (BLA) and by reducing the energy difference between aromatic and quinoid canonical structures such as in the case of polyisothianaphthenes and soluble derivatives.[10] One successful strategy to achieve narrow-band-gap π-conjugated systems is based on the pioneering work by Havinga and co-workers[11,12] and involves the alternation of electron-rich (donor, D) and electron-deficient (acceptor, A) units along the same conjugated chain.

Thieno[3,4-*b*]pyrazines have been shown to be excellent precursors for the production of low-band-gap conjugated polymers.[8,13−16] However, for these compounds to be fully utilized in optoelectronic applications, a general synthetic route must be developed that allows access to a large number of different functionalities in the 2-, 3-, 5-, and 7-positions. Such functionalities are necessary to tune and modulate the physical, electronic, and optical properties of the polymers.[14,17]

The goal of this research work was to synthesize thieno[3,4-*b*]pyrazine-based polymers, belonging to the quinoid family of low-band-gap polymers. A new narrow-band-gap system was designed, symbolized as $[-A-Q-A-]_n$, where A is aromatic donor unit and Q is *o*-quinoid acceptor unit. The properties of polymers are considered to correlate straightforwardly to those of structurally defined monomers [A−Q−A].

Herein, we report synthesis and properties of a series of thienopyrazine-based poly(heteroarylenevinylene)s (PHAVs) (**P-1**−**P-6**) by Horner polycondensation route[18] and cyano-PHAVs (**P-7**−**P-9**) by Knoevenagel polycondensation,[19] suitable for the synthesis of well-defined strictly alternating copolymers. The molecular structures of the PHAVs are shown in Schemes 1 and 2. With these synthetic routes, we obtained the PHAVs and CN-PHAVs polymers with high purity and good solubility. The optical and electrochemical properties of the PHAVs and CN-PHAVs are systematically described. To the best of our knowledge, these are first thienopyrazine-based poly(heteroarylenevinylene)s.

Results and Discussion

Synthesis of Monomers and Polymers. Synthetic routes of the monomers and polymers are shown in Schemes 1 and 2. Monomers (**M-1**−**M-4**) of the PHAVs were synthesized in a multistep synthesis. Starting from commercially available hydroquinone, in four steps 4-formyl-2,5-bis(hexyloxy)phenylboronic acid (**5**) was obtained. Similarly, 5,7-dibromo-2,3-disubsituted thieno[3,4-*b*]pyrazines (**12**−**14**) were synthesized by a modified procedure in high yields (see Supporting Information). By Suzuki coupling[20] of **5** and **15** with respective 5,7-dibromo-2,3-disubsituted thieno[3,4-*b*]pyrazines (**12**−**14**), final products (**M-1**−**M-4**) were obtained in quantitative yields. Similarly, the phosphonate esters (**M-5**−**M-7**) and dinitrile monomer (**M-8**) were synthesized by known procedures. The chemical structure of the polymers (**P-1**−**P-9**) was confirmed by FTIR, ^{1}H NMR, ^{13}C NMR, and elemental analysis. 1H NMR data were consistent with the proposed structure of the polymers. Compared with the ^{1}H NMR peaks of monomers, those of the polymers were broadened. The ^{1}H NMR spectrum of **P-1** in $CDCl_3$ showed peaks indicating two protons of phenyl rings

[†] Friedrich-Schiller-Universität Jena.
[‡] Thüringisches Institut für Textil- und Kunststoff-Forschung Rudolstadt.
* Corresponding authors. E-mail: Elisabeth.Klemm@uni-jena.de, Raja.Shahid.Ashraf@uni-jena.de.

10.1021/ma061231e CCC: $33.50
Published on Web 10/18/2006

Scheme 1. Synthesis of Monomers M-1−M-4 and Polymers P-1−P-9[a]

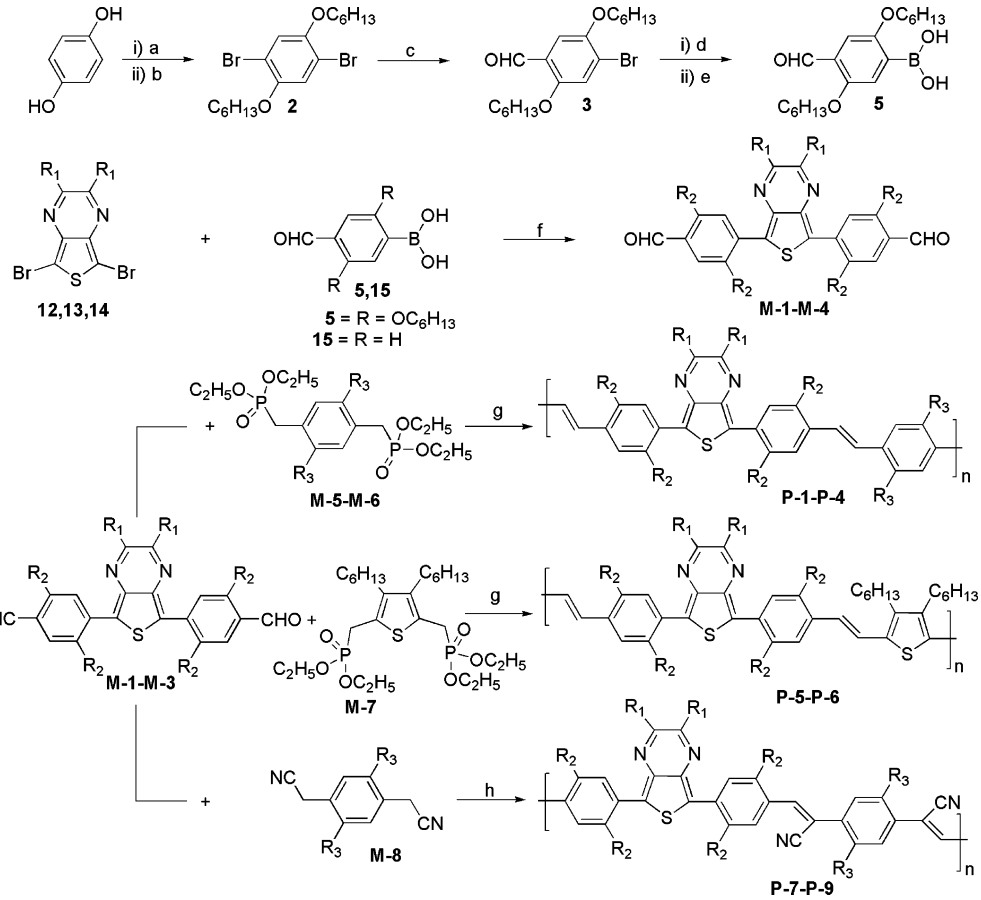

[a] Reagents and conditions: (a) 1-bromohexane, DMSO, KOH, room temperature; (b) CCl_4, bromine, room temperature; (c) diethyl ether, BuLi, DMF, 10−15 °C; (d) toluene, 1,3-propandiol, $BF_3{\cdot}OEt_2$, 6 h reflux; (e) (i) THF, BuLi, trimethylborate, −78 °C to room temperature, (ii) 1 M HCl, room temperature, 24 h; (f) toluene, THF, aqueous K_2CO_3 (2 M), $Pd(PPh_3)_4$, 80 °C, 12 h; (g) toluene, *t*-BuOK, 110 °C, 4 h; (h) THF, *t*-BuOK, *t*-BuOH, 50 °C, 4 h.

Scheme 2. Synthesis of Monomer M-7 and Model Compounds MD-1−MD-3[a]

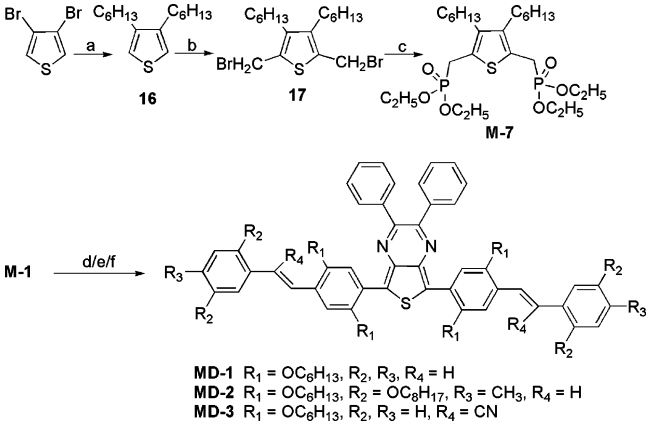

[a] Reagents and conditions: (a) (i) diethyl ether, Mg, 1-bromohexane, reflux, 2 h, (ii) $Ni(dppp)Cl_2$, 0 °C to reflux, 24 h; (b) formaldehyde, aqueous HBr, glacial CH_3COOH, room temperature, 24 h; (c) triethyl phosphite, 160 °C, 4 h; (d) diethyl benzylphosphonate, THF, *t*-BuOK, 0 °C to room temperature 3 h; (e) **20**, THF, *t*-BuOK, 0 °C to room temperature 3 h; (f) phenylacetonitrile, THF, *t*-BuOK, *t*-BuOH, 40 °C, 4 h.

adjacent to thienopyrazine (5,7-position) at $\delta = 9.00$ ppm, while protons of phenyl rings of the thienopyrazine unit along two protons of phenyl rings adjacent to the thienopyrazine moiety, vinylene and phenyl protons between $\delta = 7.63-7.26$ ppm and phenyl protons at $\delta = 6.89$ ppm, respectively; that of $-OCH_2$ protons alkoxy side chain of phenyl units appeared between $\delta = 4.29-4.15$ ppm, and other alkoxy side chain protons signals were present at $\delta = 2.06-0.93$ ppm. Similarly, the ^1H NMR spectrum of **P-3** in $CDCl_3$ showed peaks indicating protons of the thienopyrazine unit at $\delta = 8.57$ ppm and phenyl rings adjacent to thienopyrazine at $\delta = 8.42$ ppm, while other protons of phenyl rings adjacent to the thienopyrazine moiety at $\delta = 7.59$ ppm, vinylene and phenyl protons between $\delta = 7.34-6.87$ ppm; that of $-OCH_2$ protons alkoxy side chain of phenyl units appeared between $\delta = 4.20-4.12$ ppm, and other alkoxy side chain protons signals were present at $\delta = 1.93-0.88$ ppm. The ^1H NMR spectrum of **P-6** in $CDCl_3$ showed peaks indicating protons of the thienopyrazine unit at $\delta = 8.57$ ppm, phenyl rings adjacent to thienopyrazine at $\delta = 8.45$ ppm, and vinylene protons at $\delta = 7.56-7.52$ and $\delta = 7.25-7.21$ ppm, while other protons of phenyl rings adjacent to thienopyrazine moiety at $\delta = 7.17$ ppm; that of $-OCH_2$ protons alkoxy side chain of phenyl units appeared at $\delta = 4.20$ ppm, the $-CH_2$ protons of alkyl side chain of thiophene appeared at $\delta = 2.69$ ppm, and other alkyl and alkoxy side chain protons signals were present at $\delta = 2.00-0.83$ ppm. (For detailed NMR data of other polymers, see experimental, ^1H NMR, and ^{13}C NMR spectra in the Supporting Information.)

To get further information about structure and property relationship of polymers, model compounds **(MD-1−MD-3)** have been synthesized, and the chemical structures were confirmed by NMR, mass, and elemental analysis (for NMR spectra see the Supporting Information).

Table 1. Substitution of Monomers M-1−M-4 and Polymers P-1−P-9

monomer/ polymer	R^1	R^2	R^3
M-1	phenyl	OC_6H_{13}	
M-2	H	OC_6H_{13}	
M-3	ethylhexyloxybenzene	H	
M-4	phenyl	H	
P-1	phenyl	OC_6H_{13}	OC_8H_{17}
P-2	phenyl	OC_6H_{13}	ethylhexyloxy
P-3	H	OC_6H_{13}	OC_8H_{17}
P-4	ethylhexyloxybenzene	H	OC_8H_{17}
P-5	phenyl	OC_6H_{13}	
P-6	H	OC_6H_{13}	
P-7	phenyl	OC_6H_{13}	OC_8H_{17}
P-8	H	OC_6H_{13}	OC_8H_{17}
P-9	ethylhexyloxybenzene	H	OC_8H_{17}

Table 2. GPC Data of Polymers[a]

polymer	$\bar{M}_n$ (g/mol)	$\bar{M}_w$ (g/mol)	PDI	$\bar{P}_n$	yield (%)
P-1	32 100	65 100	2.0	26	72
P-2	33 500	53 100	1.5	27	70
P-3	29 200	64 600	2.2	27	65
P-4	15 600	34 200	2.1	14	54
P-5	10 000	13 300	1.5	09	54
P-6	13 300	19 200	1.4	13	50
P-7	50 200	279 000	5.0	39	71
P-8	42 200	140 000	3.3	37	67
P-9	10 500	14 000	1.9	09	57

[a] $\bar{M}_n$, GPC (polystyrene standards).

The average molecular weights of polymers were determined by gel permeation chromatography (GPC) with polystyrene as standards. THF served as eluting solvent. The number-average molecular weight $\bar{M}_n$ values of polymers (**P-1**−**P-9**) were between 50 200 and 10 000 g/mol, leading to degree of polymerization between 39 and 9 (see Table 2).

We investigated the thermal properties of these copolymers by thermogravimetric analysis (TGA) and differential scanning calorimetry (DSC) at a heating rate of 10 K/min. All the polymersare thermally stable, and thermal decomposition starts at >300 °C. We did not detect any possible phase transition signals during repeated heating/cooling DSC cycles for polymers (**P-1**−**P-9**). Obviously, the thermal stability of the PHAVs and CN-PHAVs is adequate for their applications in polymer solar cells and other optoelectronic devices.

Optical Properties. The photophysical characteristics of the new monomers, model compounds, and polymers were investigated by UV−vis absorption and photoluminescence in dilute chloroform solution as well as in the solid state. The optical data are summarized in Table 3, namely the absorption peak maxima, λ_a, the absorption coefficients at the peak maxima, log ϵ, the optical band gap energy, E_g^{opt} (calculated from $\lambda_{10\%max}$, wavelength at which the absorption coefficient has dropped to 10% of the peak value),[21] the emission maxima λ_e, and the fluorescence quantum yields, Φ_{fl}. All emission data given here were obtained after exciting at the wavelength of the main absorption band. Figures 2−4 show the absorption and emission spectra of monomers and model compounds.

The absorption spectra of the monomers (**M-1**−**M-4**) show two peaks located in the UV and visible region from ∼358 to ∼ 525 nm.The absorption maxima of monomers **M-1** and **M-2** are red-shifted relative to **M-3** and **M-4** due to presence of electron donor alkoxyphenylene adjacent to thienopyrazine moiety (see Figure 1). This indicates the substituent effect is more pronounced at the 5- and 7-positions of thieno[3,4-*b*]-pyrazine. The presence of strong donor groups at these positions lead to a red shift in absorption spectra. The absorption maxima of model compounds **(MD-1**−**MD-3)** are red-shifted relative to monomers (see Figures 3 and 4). Obviously, increase in conjugation length is the reason for this red shift. In comparison to monomers and model compounds, the respective polymers (**P-1**−**P-9**) show a red-shift in the UV absorption maxima (see Figures 5 and 7). The differences in absorption can be probably due to higher number of repeating units of polymers **P-1**−**P-9** and hence an increase in effective conjugation length.[22] The copolymers, **P-5** and **P-6**, show the lowest energy absorption peak at a longer wavelength than the polymers (**P-1**−**P-4, P-7**−**P-9**) presumably owing to the presence of the strong electron-donating alkylthiophene units to give an enhanced intermolecular CT (charge transfer) interaction in these copolymers. However, in the case of polymers **P-4** and **P-9** due to the presence of phenyl instead of alkoxyphenyl or alkylthiophene adjacent to thienopyrazine, a blue shift was observed relative to other polymers. The polymers **P-1**−**P-9** show a strong red shift of λ_{max} (∼29−61 nm) when spin-cast into thin films on quartz substrate from a chlorobenzene solution (see Figure 7). This indicates enhanced interchain interactions due to stacking of the polymers in the solid state, possibly assisted by planarization and with it an increase of conjugation length.[23] As anticipated, the alternation of electron-rich alkoxyphenylene/alkylthiophene and electron-deficient thienopyrazine units along conjugated backbone results in a low optical band gap (∼1.56−2.08 eV).

The emission maxima of **P-1**, **P-2**, and **P-6** in dilute chloroform solution are at $\lambda_{max,em} \sim 705$ nm, while the emission curves of **P-3**, **P-4**, and **P-5**, showing their maxima at $\lambda_{max,em} = 690$, 665, and 726 nm, respectively. The fluorescence quantum yields were found to be around 03−33% for **P-1**−**P-9**. The emission maxima of polymers **P-1**−**P-9** (except for **P-6**, no emission was observed) in solid film are red-shifted than in solution, and a lower fluorescence quantum yield around 01−10% is observed (Figures 6 and 8). We assumed that the reason for the low photoluminescence (PL) efficiency is a $\pi-\pi$ stacking of the conjugated backbone cofacial to each other due to the favorable interchain $\pi-\pi$ interactions, which lead to a self-quenching process of the excitons.[24−26]

Aggregate Formation in Solvent/Nonsolvent Solution. To obtain further information on the assumed self-assembly of these polymers and aggregation, the absorption and emission spectra of polymers **P-1, P-2**, and **P-8** in chloroform/methanol mixtures with different volume concentrations of methanol are shown in Figures 9, 10, and 11, respectively. It should be noted here that in all cases the bulk solution maintains homogeneity. With an increase of methanol concentration, the second absorption band of these polymers is red-shifted. Addition of methanol to the chloroform solution of **P-1, P-2**, and **P-8** led to a change in the λ_{max} and above 50 vol % of methanol; a decrease in the intensity of the first band and a shift in second band at higher wavelength were observed. Clearly, the presence of a significant amount of nonsolvent (methanol) in solution makes solute−solvent interaction energetically less favorable, thereby forcing polymer chain segments to approach each other for aggregate formation. The aggregate band in solution occurred at nearly the same wavelength as that in the spin-cast film of these polymers, clearly showing that the aggregation retained in the film state once formed in solution. Similar phenomena were found in chloroform/methanol solutions of many conjugated polymers.[27]

Electrochemical Studies. The cyclic and square-wave voltammetry were carried out using thin films of polymers prepared from dichloromethane (5 mg/mL) in acetonitrile at a potential scan rate of 15 mV/s. Ag/AgCl served as the reference electrode; it was calibrated with ferrocene ($E^{1/2}_{ferrocene} = 0.52$ V vs Ag/

Table 3. Optical Data of P-1−P-9 in Dilute $CHCl_3$ Solution (~10^{-7} M) and in Solid State[b]

		UV−vis (λ_a, nm)		E_g^{opt} [c] (eV)			PL[d] (λ_e, nm)		% Φ_{fl}	
polymer	$CHCl_3$ (log ϵ)[a]	$\lambda_{0.1max}$	film[b]	$\lambda_{0.1max}$	$CHCl_3$	film	$CHCl_3$	film	$CHCl_3$	film
P-1	446, 589 (4.5) (4.2)	690	462, 650	750	1.80	1.65	706	772	07	1
P-2	446, 592 (4.6) (4.5)	689	450, 624	735	1.80	1.69	705	738	09	1
P-3	437, 552 (4.5) (4.4)	659	448, 608	721	1.88	1.72	690	742	07	1
P-4	422, 553 (4.7) (4.3)	659	428, 582	685	1.88	1.81	665	713	17	1
P-5	465, 615 (4.5) (4.5)	718	468, 650	790	1.72	1.57	726	785	03	0
P-6	458, 585 (4.5) (4.5)	689	467, 645	795	1.80	1.56	703	000	03	0
P-7	434, 573 (4.3) (4.3)	662	449, 614	721	1.87	1.72	677	722	07	5
P-8	432, 550 (4.4) (4.5)	638	435, 596	713	1.94	1.74	658	682	20	5
P-9	387, 511 (4.4) (3.9)	592	384, 518	596	2.09	2.08	619	627	33	10

[a] Molar absorption coefficient. Molarity is based on the repeating unit. [b] Spin-coated from chlorobenzene solution. [c] $E_g^{opt} = hc/\lambda_{0.1max}$. [d] Photoluminescence data.

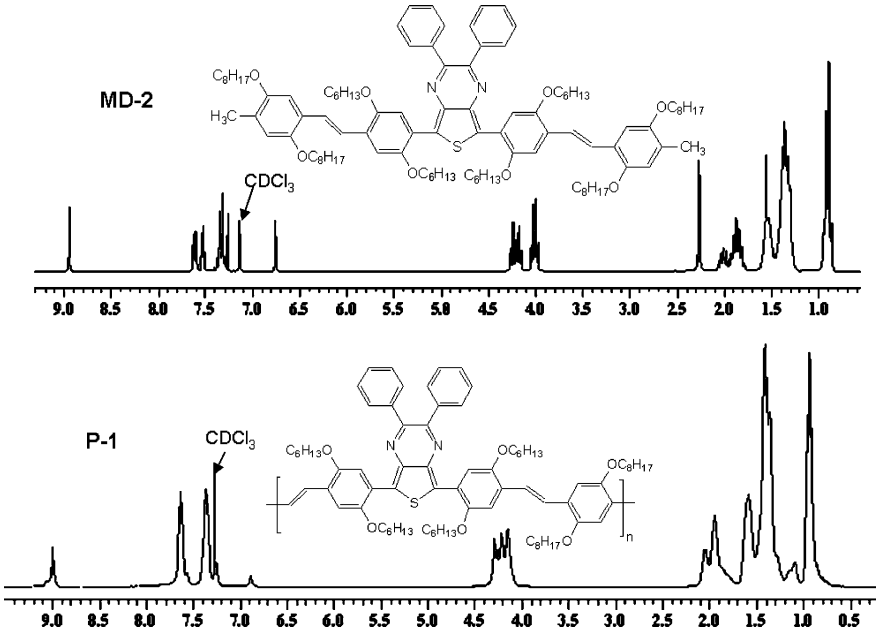

Figure 1. ^{1}H NMR spectra of **MD-2** and **P-1**.

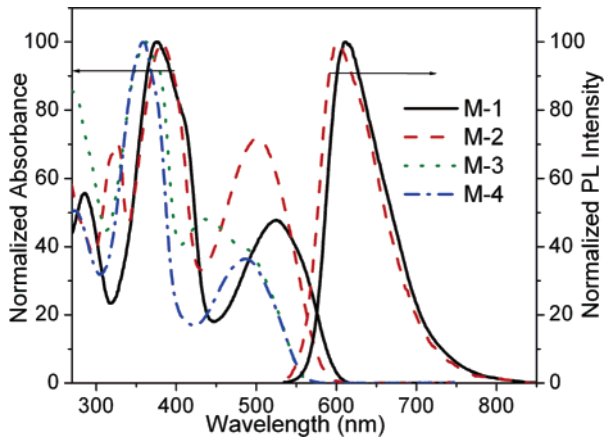

Figure 2. UV−vis spectra of **M-1**−**M-4** and emission spectra of **M-1** and **M-2** in solution ($CHCl_3$ 10^{-7} mol).

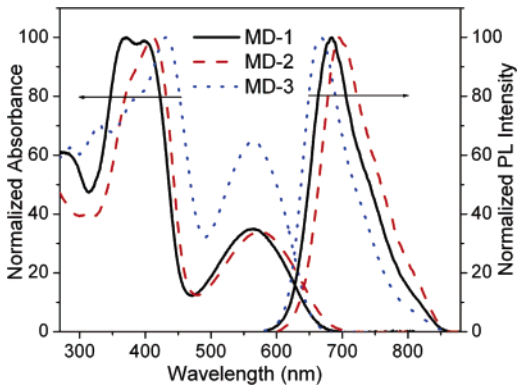

Figure 3. Normalized UV−vis and emission spectra of **MD-1**−**MD-3** in solution ($CHCl_3$ 10^{-7} mol).

AgCl). The supporting electrolyte was tetrabutylammonium hexafluorophosphate (n-Bu_4NPF_6) in anhydrous acetonitrile (0.1 M). The onset potentials are the values obtained from the intersection of the two tangents drawn at the rising current and the baseline charging current of the CV curves. Several ways to evaluate HOMO and LUMO energy levels from the onset potentials, $E^{ox/onset}$ and $E^{red/onset}$, have been proposed in the

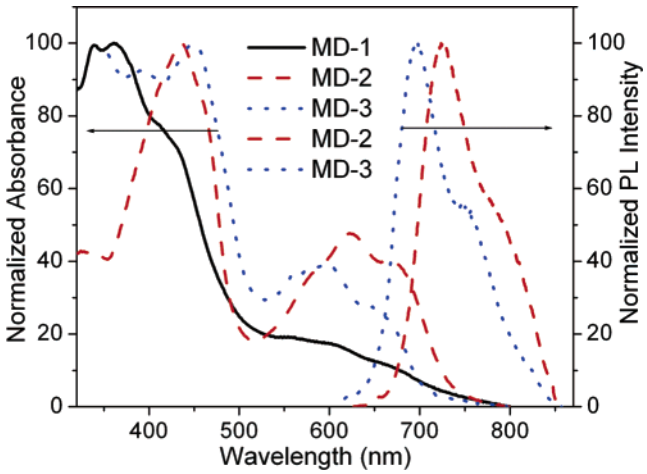

Figure 4. Normalized UV−vis of **MD-1**−**MD-3** and emission spectra of **MD-2** and **MD-3** in solid state (film from chlorobenzene).

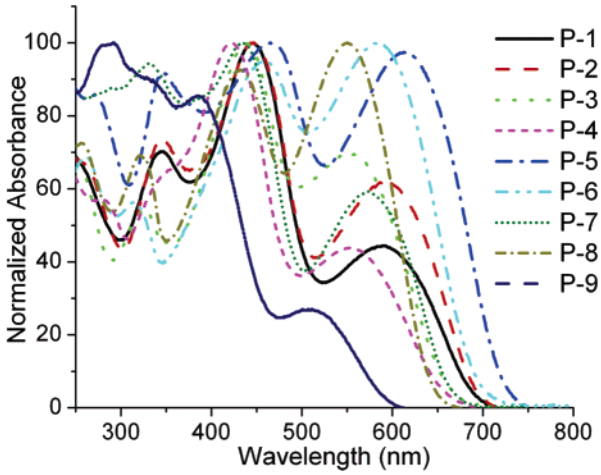

Figure 5. Normalized UV−vis spectra of **P-1**−**P-9** in solution ($CHCl_3$ 10^{-7} mol).

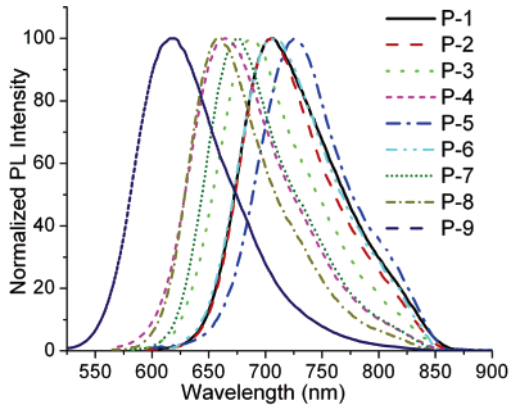

Figure 6. Normalized emission spectra of **P-1**−**P-9** in solution ($CHCl_3$ 10^{-7} mol).

literature.[28−35] These were estimated here on the basis of the reference energy level of ferrocene (4.8 eV below the vacuum level)[31,32] according to the following equation:

$$E^{\text{HOMO/LUMO}} = [-(E_{\text{onset (vs Ag/AgCl)}} - E_{\text{onset (Fc/Fc+ vs Ag/AgCl)}})] - 4.8 \text{ eV}$$

The onset and the peak potentials, the electrochemical band gap energy, and the estimated position of the upper edge of the valence band (HOMO) and of the lower edge of conduction band (LUMO) are listed in Table 4.

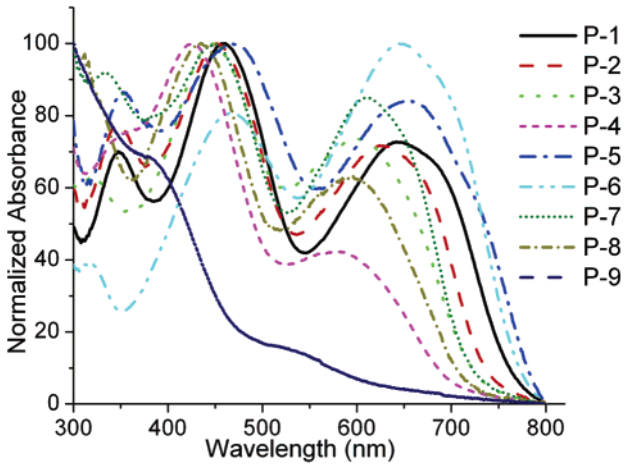

Figure 7. Normalized UV−vis spectra of **P-1**−**P-9** in solid state (film from chlorobenzene).

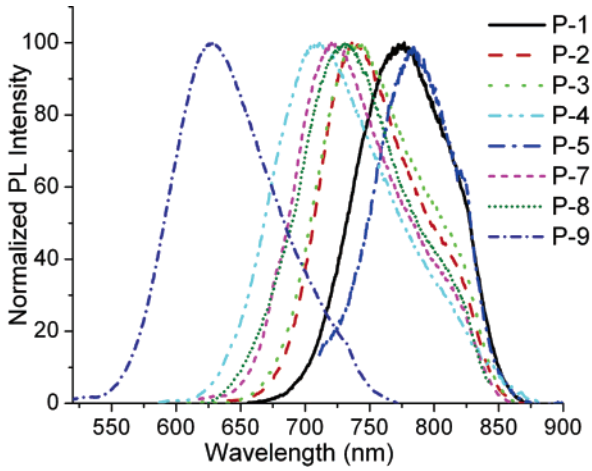

Figure 8. Normalized emission spectra of **P-1**−**P-9** (except **P-6**) in solid state (film from chlorobenzene).

All the electrochemical data for the polymers (**P-1**−**P-3, P-5**, and **P-6**) obtained from the films are listed in Table 3. As shown by the cyclic voltammograms in Figure 12, the electrochemical oxidation (or p-doping) of **P-1** starts at about 0.81 V Ag^+/Ag and gives p-doping peak at 1.04 V vs Ag^+/Ag. In a range from 0.0 to 2.0 V vs Ag^+/Ag, the film revealed stable in repeated scanning of CV, giving the same CV curves. Similarly, the oxidation of **P-2** and **P-3** starts at about 0.89 and 0.86 V vs Ag^+/Ag and gives p-doping peaks at 1.15 and 1.25 V vs Ag^+/Ag, respectively. However, oxidation of polymers **P-5** and **P-6** starts at 0.64 and 0.70 V vs Ag^+/Ag and gives peaks at 0.83 and 0.93 V, respectively. Similarly, the reduction of **P-2**, **P-3**, **P-5**, and **P-6** starts at about −1.17, −0.91, −1.19, and −1.26 V vs Ag^+/Ag and gives n-doping peaks at −1.36, −1.09, −1.39, and −1.42 V vs Ag^+/Ag, respectively. In a range from 0.0 to −2.2 V vs Ag^+/Ag, the films revealed stable in repeated scanning of CV, giving the same CV curves. However, we were not able to determine reduction in the case of **P-1**. These moderately negative reduction potentials have been attributed to the electron-withdrawing effects of the thieno[3,4-*b*]pyrazine moiety.[36] The band-gap energy directly measured from CV ($E_{g,ec/onset}$ between 1.61 and 2.06 eV) and the optical band-gap energy are close to each other. The discrepancy (ΔE_g) of both values lies within the range of error. From the onset potentials, HOMO and LUMO energy levels were estimated. These values

Table 4. . Electrochemical Potentials and Energy Levels of the Polymers P-1−P-5, P-7 and Model Compounds (MD-1−MD-3)

	oxidation potential		reduction potential		energy levels[b]		band gap	
polymer	E_{ox}[a] (V vs Ag/Ag$^+$)	$E_{onset,Ox}$ (V vs Ag/Ag$^+$)	E_{red}[a] (V vs Ag/Ag$^+$)	$E_{onset,Red}$ (V vs Ag/Ag$^+$)	HOMO (eV)	LUMO (eV)	E_g^{ec}	E_g^{opt}
P-1	1.04	0.81			-5.10	-3.49[a]	1.61	1.65
P-2	1.15	0.89	−1.36	−1.17	−5.17	−3.11	2.06	1.68
P-3	1.25	0.86	−1.09	−0.91	−5.15	−3.38	1.77	1.72
P-5	0.83	0.64	−1.39	−1.19	−4.93	−3.10	1.83	1.55
P-6	0.93	0.70	−1.42	−1.26	−4.99	−3.03	1.96	1.56
MD-1	0.92	0.82	−1.07	−0.90	−5.11	−3.39	1.72	1.83
MD-2	0.85	0.78	−0.81	−0.73	−5.07	−3.56	1.51	1.72
MD-3	1.19	1.05	−0.91	−0.78	−5.34	−3.51	1.83	1.79

[a] Reduction and oxidation potential measured by cyclic voltammetry. [b] Calculated from the reduction and oxidation potentials assuming the absolute energy level of ferrocene/ferrocenium to be 4.8 eV below vacuum.

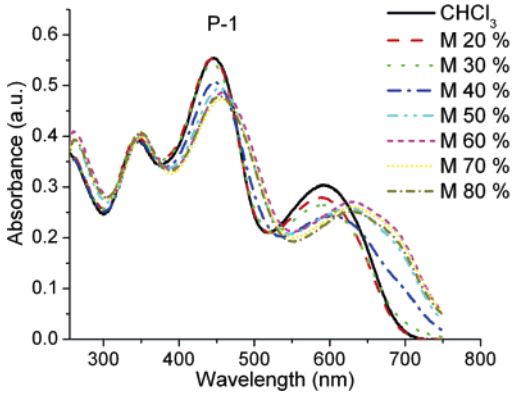

Figure 9. UV−vis spectra of **P-1** in $CHCl_3$ with different concentration of methanol (M).

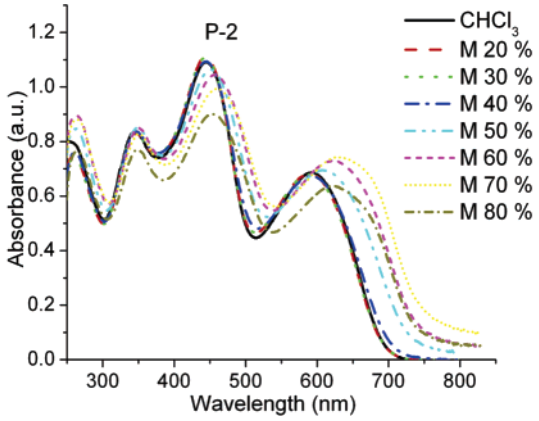

Figure 10. UV−vis spectra of **P-2** in $CHCl_3$ with different concentration of methanol (M).

indicate these polymers can be good hole-transporting materials, making them suitable candidate for hole injection and transport (Figure 13).

Figure 13 shows the HOMO and LUMO energy levels of these polymers in comparison to that of well-known electron-transporting material PCBM. From this figure we can assume that these polymers can be good hole-transporting materials in photovoltaic devices. Moreover, their broad UV absorption spectra between 400 and 700 nm make them suitable candidates to harvest more photons. Recently, we have reported photovoltaic devices of low-band-gap thieno[3,4-*b*]pyrazine-based conjugated polymers showing efficiencies up to 2.37%,[37] which is the best among low-band-gap materials. Compared to those polymers reported before, in these polymers the valley between 400 and 500 nm is reduced and shows better absorption is this range as well. Studies relating photovoltaic devices based on these novel materials are underway and will be reported soon somewhere else.

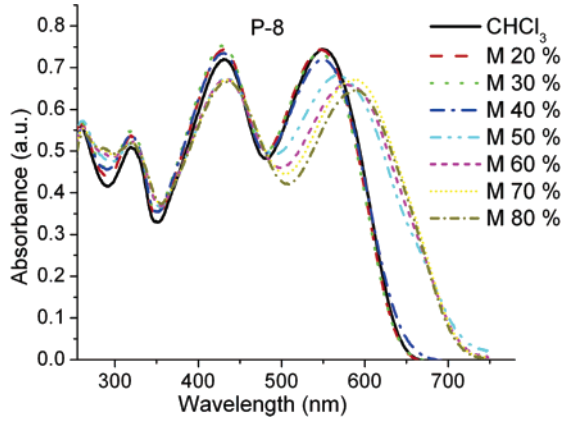

Figure 11. UV−vis spectra of **P-8** in $CHCl_3$ with different concentration of methanol (M).

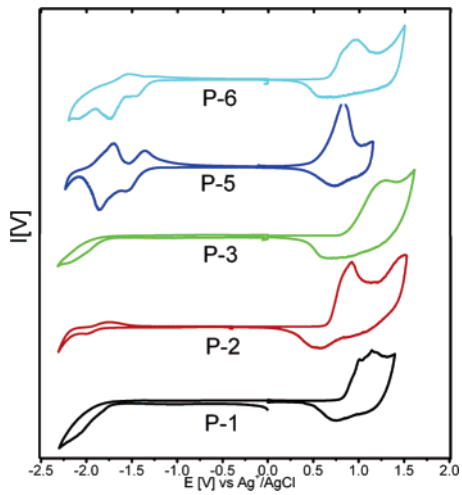

Figure 12. Cyclic voltammetry curves of polymers (**P-1**−**P-5**) in 0.1 M $TBAPF_6/CH_3CN$ at 25 °C.

We have also measured the electrochemical data for model compounds in dichloromethane solution. All the three model compounds (**MD-1**, **MD-2**, and **MD-3**) show reversible oxidation and reduction peaks (see Supporting Information, Figure S 27). The data are comparable to that of polymers. In Figure 12 and S 27 there are reversible p-doping/dedoping (oxidation/rereduction) processes at positive potential range and n-doping/dedoping (reduction/reoxidation) processes at negative potential range for all the polymers. After repeated cycles of the potential scan, the reproducibility of the cyclic voltammograms is very good, which definitely verifies the reversibility of the p-doping/dedoping and n-doping/dedoping processes. For the application of conjugated polymers and oligomers to electrochemical capacitors (ECCs), the reversible p-doping and n-doping

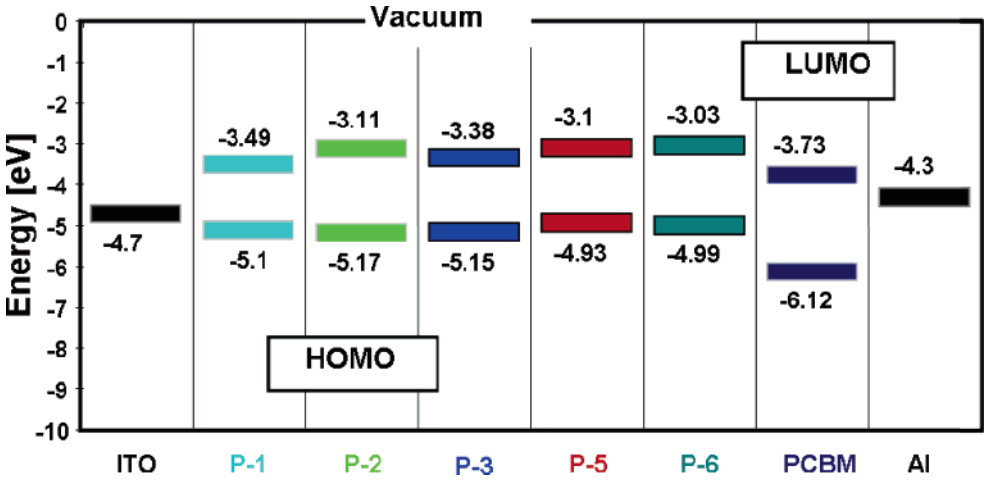

Figure 13. Energy levels of the polymers (**P-1**−**P-3, P-5**, and **P-6**) and PCBM.

processes are both needed. The reversible p-doping and n-doping properties of the polymers studied here indicate that these polymers and model compounds could also be promising materials for ECCs.

Conclusions

Novel low-band-gap thienopyrazine-based poly(heteroarylenevinylene)s (PHAVs) (**P-1**−**P-6**) by Horner polycondensation route and cyano-PHAVs (**P-7**−**P-9**) by Knoevenagel polycondensation were prepared and characterized by NMR, FTIR, and elemental analysis. Absorption and fluorescence spectra in solution and solid state revealed the optical properties of these polymers. Their UV−vis is different in the solid state of that in solution; the red shift indicates the π-stacking in the solid state. Furthermore, the addition of methanol to chloroform solution of these polymers caused the formation of a colloidal solution of π-stacked PHAVs (**P-1**, **P-2**, and **P-8**) due to self-assembly, resulting in ordered structures. The results of the cyclic voltammetry display that the p-doping/dedoping and n-doping/dedoping processes of polymers **P-1**−**P-3, P-5**, and **P-6** and model compounds **MD-1**−**MD-3** are reversible. The HOMO and LUMO energy levels and energy gap of the polymers were calculated from the electrochemical measurements.

Experimental Section

General Considerations. Materials. All starting materials were purchased from commercial suppliers (Fluka, Merck, and Aldrich). Toluene, tetrahydrofuran, and diethyl ether were dried and distilled over sodium and benzophenone. Diisopropylamine was dried over KOH and distilled. If not otherwise specified, the solvents were degassed by sparkling with argon or nitrogen 1 h prior to use. 1,4-Dialkoxybenzene (**1**),[38] 1,4-dialkoxy-2,5-dibromobenzene **(2)**,[39] 4-bromo-2,5-bis(dialkoxy)benzaldehyde **(3)**,[40] 2,5-dibromothiophene (**6**),[41] 2,5-dibromo-3,4-dinitrothiophene (**7**),[42] 3,4-diaminothiophene hydrochloride (**8**),[42] 4-formylphenylboronic acid **(15),**[43] 3,4-dihexylthiophene (**16**),[27] [4-(diethoxyphosphorylmethyl)-2,5-bis(octyloxy)-benzyl]phosphonic acid diethyl ester (**M-5**),[38] [4-(diethoxyphosphorylmethyl)-2,5-bis(2-ethylhexyloxy)benzyl]phosphonic acid diethyl ester (**M-6**),[38] and (4-cyanomethyl-2,5-bis(octyloxy)phenyl)acetonitrile (**M-8**)[44] were prepared according to known literature procedures.

Methods. ^{1}H NMR and ^{13}C NMR spectra were obtained in deuterated chloroform using a Bruker DRX 400 and a Bruker AC 250. Chemical shifts (δ values) are given in parts per million with tetramethylsilane as an internal standard. Elemental analysis was measured on a CHNS-932 Automat Leco. Infrared spectroscopy was recorded on a Nicolet Impact 400. A NETZSCH instrument served for the thermogravimetric measurements. Gel permeation chromatography (GPC) was performed on a set of Knauer using THF as eluent and polystyrene as a standard. The absorption spectra were recorded in dilute chloroform solution (10^{-5}−10^{-6} M) on a Perkin-Elmer UV/vis-NIR spectrometer Lambda 19. Quantum-corrected emission spectra were measured in dilute chloroform solution (10^{-6} M) with an LS 50 luminescence spectrometer (Perkin-Elmer). Photoluminescence quantum yields were calculated according to Demas and Crosby[45] against quinine sulfate in 0.1 N sulfuric acid as a standard (ϕ_{fl} = 55%). The solid-state absorption and emission were measured with a Hitachi F-4500. The films were cast from chlorobenzene. The quantum yield in the solid state was determined against a CF_3P−PPV (poly{1,4-phenylene-[1-(4-trifluoromethylphenyl)ethenylene]-2,5-dimethoxy-1,4-phenylene-[2-(4-trifluoromethylphenyl)ethenylene]}) copolymer reference that has been measured by integrating sphere as 0.43. The cyclic voltammogram was recorded on a computer-controlled EG&G potentiostat/galvanostat model 283. The lowest unoccupied molecular orbital (LUMO) and the highest occupied molecular orbital (HOMO) energy levels of the polymers were converted from the onset reduction and oxidation potentials, respectively, with the assumption that the energy level of ferrocene/ferrocenium (Fc) is 4.8 eV below vacuum.

2-(4-Bromo-2,5-bis(hexyloxy)phenyl)-[1,3]dioxane (4). To a solution of 4-bromo-2,5-bis(dialkoxy)benzaldehyde **(3)** (10 g, 25.95 mmol) and propane-1,3-diol (2.2 g, 28.8 mmol) in toluene (30 mL) was added BF_3·OEt_2 (3−4 drops). This mixture was refluxed for 6−7 h in a Dean Stark apparatus to remove the theoretical amount of water. The solution was washed with 1 M aqueous $NaHCO_3$ and then with water, dried over $MgSO_4$, and concentrated in a vacuum to give **5** (10.8 g, 94%) as a white solid, which was sufficiently pure to be employed in the next step.

4-Formyl-2,5-bis(hexyloxy)phenylboronic Acid (5). A 2.5 M solution of *n*-butyllithium (11.3 mL, 28.4 mmol) was added to an argon-purged solution of 2-(4-bromo-2,5-bis(hexyloxy)phenyl)-[1,3]-dioxane **(4)** (10.5 g, 23.7 mmol) in anhydrous THF (50 mL) at −78 °C using a syringe. The solution was then stirred for 2 h. Trimethyl borate (3 g, 28.4 mmol) was added with a syringe. The resulting mixture was allowed to come to room temperature and stir for 24 h. Then it was cooled to 0 °C, 2 N HCl (43 mL) was added, and the mixture was at room temperature for an additional 20 h. The organic layer was separated and the aqueous layer was extracted with (3 × 50 mL) diethyl ether. The combined ether layers were washed twice with 50 mL of water and brine and dried over magnesium sulfate. After filtration, solvent was then removed under reduced pressure. The crude product was purified by recrystallization from hexane to give a light yellow powder. Yield: 6.3 g (76%). ^{1}H NMR (250 MHz, $CDCl_3$): δ = 10.50 (s, 1H), 7.50 (s, 1H), 7.32 (s, 1H), 6.46 (bs, 2H), 4.09 (t, 2H), 3.95 (t, 2H), 2.16−0.88 (m, 22H). ^{13}C NMR (62 MHz, $CDCl_3$): δ = 190.33, 157.74,

155.88, 127.23, 121.27, 108.89, 69.29, 31.65, 31.57, 29.32, 29.27, 25.86, 25.77, 22.70, 22.64, 14.13, 14.08. Elemental analysis calculated for $C_{19}H_{31}BO_5$ (350.26 g/mol): C, 65.15; H, 8.92. Found: C, 65.28; H, 9.09.

General Procedure for Synthesis of Monomers M-1−M-4. Under an argon atmosphere, 5,7-dibromo-2,3-disubsituted thieno-[3,4-*b*]pyrazines (**12**−**14**) (5 mmol) and 4-formyl-2,5-bis(substituted)phenylboronic acids **(5, 15)** (12.5 mmol) were added to degassed aqueous solution of potassium carbonate 16 mL (2.0 M), toluene, and THF 40 mL (1:1, volume ratio). After 30 min degassing 3 mol % (173 mg, 0.15 mmol) of $Pd(PPh_3)_4$ was added. The mixture was stirred vigorously at 80−90 °C for 24 h under an argon atmosphere. The reaction mixture was cooled to room temperature, followed by the addition toluene and water. The organic layer was separated and washed with water and brine and dried over $MgSO_4$. After evaporation of solvent, the product was further purified by chromatography (solvent, toluene). Finally, pure product can be obtained by recrystallization from hexane.

4,4′-2,3-Diphenylthieno[3,4-*b*]pyrazine-5,7-diylbis(2,5-dihexyloxybenzaldehyde) (M − 1). 5,7-Dibromo-2,3-diphenylthieno[3,4-*b*]pyrazine **(13)** (2.24 g, 5 mmol) and 4-formyl-2,5-bis(hexyloxy)-phenylboronic acid **(5) (**4.38 g, 12.5 mmol). Yield: 2.5 g (57%). ^{1}H NMR (250 MHz, CD_2Cl_2): δ = 10.54 (s, 2H), 9.23 (s, 2H), 7.58−7.31 (m, 12H), 4.27−4.13 (m, 8H), 2.02−0.87 (m, 44H). ^{13}C NMR (62 MHz, $CDCl_3$): δ = 190.64, 157.95, 153.51, 151.23, 142.21, 141.64, 139.99, 131.99, 131.47, 131.03, 130.47, 130.14, 125.28, 117.34, 113.16, 111.66, 72.06, 71.32, 33.76, 33.64, 31.49, 31.08, 27.97, 27.34, 24.77, 24.51, 15.95, 15.88. FAB MS: *m*/*z* 896 (M^+). Elemental analysis calculated for $C_{56}H_{68}N_2O_6S$ (897.22 g/mol): C, 74.97; H, 7.64; N, 3.12; S, 3.57. Found: C, 74.96; H, 7.52; N, 3.08; S, 3.46.

4,4′-Thieno[3,4-*b*]pyrazine-5,7-diyl-bis(2,5-dihexyloxybenzaldehyde) (M − 2). 5,7-Dibromo-thieno[3,4-*b*]pyrazine **(12)** (1.47 g, 5 mmol) and 4-formyl-2,5-bis(hexyloxy)phenylboronic acid **(5)** (4.38 g, 12.5 mmol). Yield: 1.7 g (68%). ^{1}H NMR (250 MHz, $CDCl_3$): δ = 10.44 (s, 2H), 8.57 (s, 4H), 7.40 (s, 2H), 4.15−3.96 (m, 8H), 1.85−0.72 (m, 44H). ^{13}C NMR (62 MHz, $CDCl_3$): δ = 188.40, 155.15, 148.49, 142.52, 140.65, 128.63, 127.97, 122.97, 115.15, 109.20, 69.09, 68.46, 30.83, 30.75, 28.42, 28.38, 25.06, 24.99, 21.85, 21.75, 13.27, 13.17. FAB MS: *m*/*z* 744.4 (M^+). Elemental analysis calculated for $C_{44}H_{60}N_2O_6S$ (745.025 g/mol): C, 70.94; H, 8.12; N, 3.76; S, 4.30. Found: C, 71.20; H, 8.26; N, 3.54; S, 4.28.

4,4′-2,3-Bis[4-(2-ethylhexyloxy)phenyl]thieno[3.4-*b*]pyrazine-5,7-diylbis(2,5-dihexyloxybenzaldehyde) (M − 3). 5,7-Dibromo-2,3-bis[4-(2-ethylhexyloxy)phenyl]thieno[3.4-*b*]pyrazine **(14)** (1.4 g, 2 mmol) and 4-formylphenylboronic acid **(15)** (1.16 g, 5 mmol). Yield: 0.8 g (56%). ^{1}H NMR (250 MHz, $CDCl_3$): δ = 10.04 (s, 2H), 8.51 (d, 4H), 7.98 (d, 4H), 7.55 (d, 4H), 6.92 (d, 4H),3.92 (d, 4H), 1.78−0.86 (m, 30H). ^{13}C NMR (62 MHz, $CDCl_3$): δ = 191.41, 160.61, 153.30, 150.78, 140.26, 138.96, 135.11, 131.37, 130.23, 129.46, 127.91, 114.33, 70.72, 39.39, 31.92, 30.55, 29.68, 29.11, 23.88, 23.03, 23.01, 22.67, 14.06, 14.04, 11.12. FAB MS: *m*/*z* 752 (M^+). Elemental analysis calculated for $C_{48}H_{52}N_2O_4S$ (753.0 g/mol): C, 76.56; H, 6.96; N, 3.72; S, 4.26. Found: C, 76.25; H, 7.26; N, 3.77; S, 4.18.

4,4′-2,3-Diphenylthieno[3,4-*b*]pyrazine-5,7-diylbis(benzaldehyde) (M − 4). 5,7-Dibromo-2,3-diphenylthieno[3,4-*b*]pyrazine **(13)** (1.34 g, 3 mmol) and 4-formylphenylboronic acid **(15)** (1.12 g, 7.5 mmol). Yield: 0.94 g (63%). ^{1}H NMR (250 MHz, $CDCl_3$): δ = 10.06 (s, 2H), 8.52 (d, 2H), 8.00 (d, 2H), 7.58−7.34 (m, 10H). FAB MS: *m*/*z* 496.1 (M^+); mp 324−325 °C. Elemental analysis calculated for $C_{32}H_{20}N_2O_2S$ (496.12 g/mol): C, 77.40; H, 4.06; N, 5.64; S, 6.46. Found: C, 77.21; H, 4.09; N, 5.49; S, 6.38.

2,5-Bis(bromomethyl)-3,4-dihexylthiophene (17). Compound **16** (10.0 g, 39.6 mmol) and paraformaldehyde (2.84 g, 94.6 mmol) were dissolved in 5 mL of acetic acid and HBr solution (30% in acetic acid, 95 mmol, 20 mL). The reaction was stirred at room temperature under argon overnight. The reaction was diluted with 200 mL of ethyl ether and washed with water, saturated $NaHCO_3$ solution, and brine. After the solvent removal, 13 g of light brown oil was obtained (75% yield), which was sufficiently pure for next step reaction.

3,4-Dihexyl-2,5-bis(methylenediethyl phosphate)thiophene (M − 7). Compound **17** (8.76 g, 20 mmol) reacted with triethyl phosphite (10 g, 60 mmol) at 120 °C for 4 h. The crude product was purified by column chromatography on silica gel using acetone−hexane (25:75) as an eluent to give 8.8 g of light yellow oil (80% yield). ^{1}H NMR (250 MHz, $CDCl_3$): δ = 4.14−4.01 (m, 8 H), 3.26−3.21 (m, 4 H), 2.46 (t, 4 H), 1.42−0.86 (m, 34 H). ^{13}C NMR (62 MHz, $CDCl_3$): δ = 139.98, 124.53, 62.26, 31.64, 30.58, 29.53, 27.25, 25.86, 22.59, 16.37, 16.05, 14.01.

Model Compounds Synthesis. MD-1. Dialdehyde **M-1** (0.5 g, 0.56 mmol) and diethyl benzylphosphonate (0.28 g, 1.2 mmol) were dissolved in dried THF (7 mL) while stirring vigorously under argon at 0 °C. Potassium *tert*-butoxide (1 M in THF, 1 mL, 1.8 mmol) was added dropwise, and the solution was stirred for a further 2 h at room temperature. The reaction was quenched by addition of water, and the aqueous layer was extracted with diethyl ether (25 mL) three times. The ether layer was washed with water and brine and dried over anhydrous $MgSO_4$. After the solvent was removed under reduced pressure, the product was purified by chromatography (solvent, dicholomethane:hexane, 2:1). Yield: 0.42 g (73%) dark violet solid. ^{1}H NMR (400 MHz, $CDCl_3$): δ = 8.97 (s, 2H), 7.61−7.20 (m, 26H), 4.27−4.15 (m, 8H), 2.04−0.87 (m, 44H). ^{13}C NMR (400 MHz, $CDCl_3$): δ = 150.98, 150.56, 149.48, 139.87, 139.01, 138.09, 129.88, 128.84, 128.62, 128.52, 127.89, 127.53, 127.33, 126.52, 125.68, 123.69, 123.45, 114.91, 110.48, 70.11, 69.20, 31.65, 29.57, 29.46, 25.98, 25.86, 22.67, 22.60, 14.03. FAB MS: *m*/*z* 1044.6 (M^+). UV−vis ($CHCl_3$): λ_{max}/nm (ϵ/(L mol^{-1} cm^{-1})) 370 (45 800), 398 (45 300), 564 (16 000). Elemental analysis calculated for $C_{70}H_{80}N_2O_4S$ (1045.46 g/mol): C, 80.42; H, 7.71; N, 2.68; S, 3.07. Found: C, 80.64; H, 8.03; N, 2.29; S, 2.84.

MD-2. Dialdehyde **M-1** (0.5 g, 0.56 mmol) and **20** (0.61 g, 1.2 mmol). Yield: 0.42 g (71%) dark green solid. ^{1}H NMR (400 MHz, $CDCl_3$): δ = 8.94 (s, 2H), 7.63−7.32 (m, 16H), 7.14 (s, 2H), 6.76 (s, 2H), 4.26−3.97 (m, 16H), 2.27 (s, 6H), 2.04−0.86 (m, 104H). ^{13}C NMR (400 MHz, $CDCl_3$): δ = 151.60, 150.77, 150.53, 150.44, 149.93, 138.91, 129.89, 128.47, 127.86, 127.58, 127.54, 126.70, 125.36, 123.90, 122.97, 122.51, 116.22, 114.90, 110.29, 109.34, 70.03, 69.78, 69.17, 68.84, 31.88, 31.83, 31.68, 31.65, 29.58, 29.47, 29.42, 29.33, 29.30, 26.20, 25.97, 25.89, 22.70, 22.66, 22.60, 16.43, 14.07, 14.01**.** FAB MS: *m*/*z* 1586 (M^+). UV−vis ($CHCl_3$): λ_{max}/nm (ϵ/(L mol^{-1} cm^{-1})) 411 (68 900), 574 (23 500). Elemental analysis calculated for $C_{104}H_{148}N_2O_8S$ (1586.36 g/mol): C, 78.74; H, 9.40; N, 1.77; S, 2.02. Found: C, 78.68; H, 9.34; N, 1.72; S, 1.93.

MD-3. Dialdehyde **M-1** (0.5 g, 0.56 mmol) and phenylacetonitrile (0.14 g, 1.2 mmol). Yield: 0.48 g (79%) dark green solid. ^{1}H NMR (400 MHz, $CDCl_3$): δ = 9.17 (s, 2H), 8.09−7.31 (m, 20H), 4.36−4.11 (m, 16H), 2.36 (s, 6H), 2.07−0.86 (m, 104H). ^{13}C NMR (400 MHz, $CDCl_3$): δ = 150.06, 148.95, 147.07, 137.87, 137.76, 134.31, 133.29, 128.01, 127.13, 127.08, 126.84, 126.32, 126.07, 124.68, 124.02, 119.79, 117.01, 112.13, 109.28, 107.62, 68.15, 67.29, 29.75, 29.72, 27.53, 27.40, 24.03, 23.93, 23.91, 20.73, 12.11, 12.06. FAB MS: *m*/*z* 1094 (M^+). UV−vis ($CHCl_3$): λ_{max}/nm (ϵ/(L mol^{-1} cm^{-1})) 329 (31 300), 431 (44 700), 564 (28 900). Elemental analysis calculated for $C_{72}H_{78}N_4O_4S$ (1095.48 g/mol): C, 78.94; H, 7.18; N, 5.11; S, 2.93. Found: C, 78.70; H, 7.20; N, 5.02; S, 2.76.

Polymer Synthesis. General Procedure for Horner−Wadsworth−Emmons Polycondensation. Dialdehyde (0.56 mmol) and the corresponding phosphonate derivative (0.56 mmol) were dissolved in dried toluene (10 mL) while stirring vigorously under argon and heating under reflux. The polycondensations was started by adding potassium *tert*-butoxide (2.23 mmol), and the solution was refluxed for a further 3.5 h. After cooling to room temperature toluene (15 mL) and an excess of dilute HCl were added. The organic layer was separated and extracted several times with distilled water until the water phase became neutral (pH = 6−7). A Dean-Stark apparatus was used to dry the organic layer. The hot (50−60 °C) toluene solution was filtered; the filtrate was concen-

trated to the minimum by using a rotary evaporator and then precipitated in vigorously stirred methanol (300 mL). The polymer was extracted (Soxhlet extractor) 12 h with methanol, acetone, and finally diethyl ether to remove oligomers and dried under vacuum. The polymer yields are mentioned after purification.

P-1. Dialdehyde **M-1** (0.5 g, 0.56 mmol) and **M-5** (0.35 g, 0.56 mmol). Yield: 0.49 g (0.401 mmol, pertaining of the repeating unit) of dark green polymer was obtained. Yield: 491 mg (72%). ^{1}H NMR (400 MHz, $CDCl_3$): δ = 9.00 (bs, 2H), 7.63−7.26 (m, 16H), 6.89 (bs, 2H), 4.29−4.15 (m, 12H), 2.06−0.93 (m, 74H). ^{13}C NMR (400 MHz, $CDCl_3$): δ = 151.04, 150.56, 150.44, 149.67, 148.86, 140.03, 139.07, 129.92, 128.49, 127.89, 127.37, 127.22, 126.73, 126.09, 125.53, 125.19, 123.74, 123.53, 123.41, 116.39, 115.12, 114.41, 110.92, 110.56, 70.19, 69.94, 69.73, 69.32, 31.89, 31.69, 31.49, 29.63, 29.55, 29.48, 29.34, 26.29, 25.98, 25.72, 22.66, 14.02. GPC (THF): $\bar{M}_w$ = 65 100 g/mol, $\bar{M}_n$ = 32 100; PDI = 2.0; $\bar{P}_n$ = 26. UV−vis ($CHCl_3$): λ_{max}/nm (ϵ/(L mol^{-1} cm^{-1})): 446 (32 300), 589 (20 000). Elemental analysis calculated for $(C_{80}H_{106}N_2O_6S)_n$ $(1223.8)_n$: C, 78.52; H, 8.71: N, 2.29; S, 2.62. Found: C, 77.35; H, 8.74,: N, 2.13; S, 2.53.

P-2. Dialdehyde **M-1** (0.5 g, 0.56 mmol) and 1,4-bis(2-ethylhexyloxy)-2,5-di(methylenediethyl phosphate)benzene **(M − 6)** (0.31 g, 0.56 mmol). Yield: 0.48 g (70%) of green polymer. ^{1}H NMR (400 MHz, $CDCl_3$): δ = 8.99 (bs, 2H), 7.63−7.26 (m, 16H), 6.88 (bs, 2H), 4.28−4.01 (m, 12H), 2.04−0.72 (m, 74H). ^{13}C NMR (400 MHz, $CDCl_3$): δ = 150.56, 150.41, 149.70, 148.86, 140.03, 139.05, 129.91, 128.48, 127.88, 127.63, 127.15, 126.78, 126.13, 125.58, 125.11, 123.34, 123.14, 122.91, 122.64, 116.40, 115.22, 114.37, 110.11, 110.02, 71.95, 71.83, 71.65, 70.06, 69.35, 69.15, 68.79, 39.92, 39.78, 39.40, 31.66, 30.95, 30.76, 30.63, 29.57, 29.25, 28.92, 25.94, 25.72, 24.38, 24.11, 23.11, 22.89, 22.66, 22.60, 14.02, 13.95. GPC (THF): $\bar{M}_w$ = 53 100 g/mol, $\bar{M}_n$ = 33 500; PDI = 1.50; $\bar{P}_n$ = 27. UV−vis ($CHCl_3$): λ_{max}/nm (ϵ/(L mol^{-1} cm^{-1})): 446 (47 000), 592 (29 100). Elemental analysis calculated for $(C_{80}H_{106}N_2O_6S)_n$ $(1223.8)_n$: C, 78.52; H, 8.73: N, 2.29; S, 2.62. Found: C, 78.15; H, 8.83,: N, 2.26; S, 2.62.

P-3. Dialdehyde **M-2** (0.5 g, 0.67 mmol) and **M-5** (0.43 g, 0.67 mmol). 0.43 g (0.440 mmol, pertaining of the repeating unit) of dark green polymer was obtained. Yield: 65%. **¹**H NMR (400 MHz, $CDCl_3$): δ = 8.57 (bs, 2H), 8.42 (bs, 2H), 7.59 (bs, 2H), 7.34−6.87 (m, 6H), 4.2−4.12 (m, 12H), 1.93−0.88 (m, 74H). ^{13}C NMR (400 MHz, $CDCl_3$): δ = 151.25, 150.89, 149.77, 142.63, 140.48, 128.36, 127.62, 127.35, 123.80, 123.37, 122.54, 115.72, 114.29, 110.73, 110.38, 69.97, 69.63, 69.46, 31.89, 31.72, 31.62, 29.61, 29.46, 29.35, 26.30, 25.99, 25.90, 22.67, 22.58, 14.07, 13.98. GPC (THF, polystyrene): $\bar{M}_w$ = 64 600 g/mol, $\bar{M}_n$ = 29 200; PDI = 2.2; $\bar{P}_n$ = 27. UV−vis ($CHCl_3$): λ_{max}/nm (ϵ/(L mol^{-1} cm^{-1})): 326 (18 200), 437 (33 300), 552 (23 400). Elemental analysis calculated for $(C_{68}H_{98}N_2O_6S)_n$ $(1071.58)_n$: C, 76.22; H, 9.22: N, 2.61; S, 2.99. Found: C, 75.40; H, 9.36,: N, 2.43; S, 2.54.

P-4. Dialdehyde **M-3** (0.5 g, 0.66 mmol) and **M-5** (0.42 g, 0.66 mmol) Yield: 0.39 g (54%) dark red polymer. ^{1}H NMR (400 MHz, $CDCl_3$): δ = 8.40−6.87 (m, 22H), 4.10−3.90 (m, 8H), 1.96−0.91 (m, 60H). ^{13}C NMR (400 MHz, $CDCl_3$): δ = 160.17, 153.17, 150.09, 139.83, 137.99, 132,87, 131.42, 130.27, 129.54, 128.78, 127.65, 126.40, 125.45, 124. 67, 116.78, 115.97, 115.30, 112.34, 111.68, 70.84, 69.91, 69.76, 69.33, 39.44, 36.61, 31.71, 30.57, 29.26, 29.11, 26.08, 23.91, 22.99, 22.60, 18.68, 13.99, 11.08. GPC (THF): $\bar{M}_w$ = 34 200 g/mol, $\bar{M}_n$ = 15 600; PDI = 2.1; $\bar{P}_n$ = 14. UV−vis ($CHCl_3$): λ_{max}/nm (ϵ/(L mol^{-1} cm^{-1})): 422 (47 800), 553 (21 000). Elemental analysis calculated for $(C_{72}H_{90}N_2O_4S)_n$ $(1079.56)_n$: C, 80.10; H, 8.40: N, 2.59; S, 2.97; Found: C, 79.38; H, 8.17,: N, 2.31; S, 2.81.

P-5. Dialdehyde **M-1** (0.5 g, 0.56 mmol) and **M-7** (0.31 g, 0.56 mmol) Yield: 0.34 g (54%) green polymer. ^{1}H NMR (250 MHz, $CDCl_3$): δ = 9.02 (s, 2H), 7.63−7.18 (m, 14H), 4.27−4.21 (m, 8H), 2.71 (t, 4H), 2.05−0.94 (m, 66H). ^{13}C NMR (62 MHz, $CDCl_3$): δ = 151.30, 150.61, 149.68, 141.51, 140.30, 139.15, 136.50, 129.91, 128.48, 127.90, 127.65, 126.91, 126.11, 124.42, 123.73, 123.18, 122,47, 114.88, 112.02, 70.28, 69.24, 31.69, 31.39, 29.66, 29.57, 29.26, 27.33, 25.91, 25.54, 22.67, 14.04, 13.97. GPC (THF): $\bar{M}_w$ = 13 300 g/mol, $\bar{M}_n$ = 1000; PDI = 1.50; $\bar{P}_n$ = 9. UV−vis ($CHCl_3$): λ_{max}/nm (ϵ/(L mol^{-1} cm^{-1})): 465 (31 100), 615 (30 300). Elemental analysis calculated for $(C_{74}H_{96}N_2O_4S_2)_n$ $(1141.7)_n$: C, 77.85; H, 8.48: N, 2.45; S, 5.62. Found: C, 77.24; H, 8.11,: N, 2.40; S, 5.29.

P-6. Dialdehyde **M-2** (0.5 g, 0.67 mmol) and **M-7** (0.37 g, 0.67 mmol) Yield: 0.33 g (50%) of blue polymer. ^{1}H NMR (400 MHz, $CDCl_3$): δ = 8.57 (bs, 2H), 8.45 (bs, 2H), 7.56−7.52 (d, 2H), 7.25−7.21 (d, 2H), 7.17 (bs, 2H), 4.2 (m, 8H), 2.69 (t, 4H), 2.00−0.83 (m, 66H). ^{13}C NMR (400 MHz, $CDCl_3$): δ = 151.18, 149.73, 142.58, 141.53, 140.55, 136.40, 128.35, 126.88, 123.57, 122.45, 122.17, 115.72, 111.84, 70.16, 69.48, 31.68, 31.58, 31.35, 29.51, 27.30, 25.92, 25.84, 22.63, 22.53, 13.99, 13.88. GPC (THF): $\bar{M}_w$ = 19 200 g/mol, $\bar{M}_n$ = 13 300; PDI = 1.40; $\bar{P}_n$ = 13. UV−vis ($CHCl_3$): λ_{max}/nm (ϵ/(L mol^{-1} cm^{-1})): 458 (31 000), 585 (33 100). Elemental analysis calculated for $(C_{62}H_{88}N_2O_4S_2)_n$ $(989.5)_n$: C, 75.26; H, 8.96: N, 2.83; S, 6.48. Found: C, 74.30; H, 8.41,: N, 2.50; S, 6.07.

General Procedure for Knoevenagel Polycondensation. Tetrabutylammonium hydroxide (62 μL, 1.0 M in methanol) was added into the degassed mixture solution of the dinitrile (0.56 mmol), the dialdehyde (0.56 mmol), THF (5 mL), and *tert*-butyl alcohol (3 mL). The reaction mixture was heated to 50 °C while stirring under a nitrogen atmosphere. After stirring for 2 h, the dark mixture was poured into methanol (150 mL), and the precipitate was collected by filtration. The crude polymer was Soxhlet extracted 12 h with methanol, acetone, and finally diethyl ether to remove oligomers and dried under vacuum. The polymer yields are mentioned after purification.

P-7. Dialdehyde **M-1** (0.5 g, 0.56 mmol) and **M-8** (0.23 g, 0.56 mmol) Yield: 0.5 g (71%) of green polymer. ^{1}H NMR (400 MHz, $CDCl_3$): δ = 9.17 (s, 2H), 8.19 (s, 2H), 7.61−7.18 (m, 14H), 4.41−4.15 (m, 12H), 2.08−0.87 (m, 74H). ^{13}C NMR (400 MHz, $CDCl_3$): δ = 151.94, 151.43, 150.79, 149.27, 140.82, 140.19, 139.80, 129.88, 129.44, 128.70, 128.33, 127.92, 126.93, 126.51, 123.18, 122.25, 118.88, 115.30, 114.78, 114.25, 112.91, 111.72, 110.09, 106.97, 71.25, 70.23, 70.02, 69.23, 31.79, 31.58, 29.38, 29.30, 29.22, 26.12, 25.87, 25.79, 22.59, 13.94. GPC (THF): $\bar{M}_w$ = 279 000 g/mol, $\bar{M}_n$ = 50 200; PDI = 5.0; $\bar{P}_n$ = 39. UV−vis ($CHCl_3$): λ_{max}/nm (ϵ/(L mol^{-1} cm^{-1})): 434 (29 500), 573 (17 400). Elemental analysis calculated for $(C_{82}H_{104}N_2O_6S)_n$ $(1273.8)_n$: C, 77.32; H, 8.23: N, 4.40; S, 2.52. Found: C, 76.92; H, 8.26,: N, 4.15; S, 2.19.

P-8: Dialdehyde **M-2** (0.5 g, 0.67 mmol) and dinitrile **M-8** (0.28 g, 0.67 mmol) Yield: 0.50 g (67%) green polymer. ^{1}H NMR (400 MHz, $CDCl_3$): δ = 8.65 (bs, 2H), 8.19−8.16 (m, 4H), 7.18 (bs, 2H), 7.05 (s, 2H), 4.33−3.75 (m, 12H), 2.00−0.82 (m, 74H). ^{13}C NMR (400 MHz, $CDCl_3$): δ = 151.86, 150.81, 149.22, 142.80, 141.12, 140.91, 128.67, 126.33, 125.81, 122.87, 118.76, 114.82, 111.85, 107.02, 70.14, 70.04, 69.42, 31.89, 31.77, 31.57, 29.30, 29.19, 26.10, 25.81, 22.57, 13.90. GPC (THF): $\bar{M}_w$ = 140 000 g/mol, $\bar{M}_n$ = 42 200; PDI = 3.3; $\bar{P}_n$ = 37. UV−vis ($CHCl_3$): λ_{max}/nm (ϵ/(L mol^{-1} cm^{-1})): 432 (29 000), 550 (31 600). Elemental analysis calculated for $(C_{70}H_{96}N_4O_6S)_n$ $(1121.62)_n$: C, 74.96; H, 8.63: N, 5.00; S, 2.86. Found: C, 74.53; H, 8.50,: N, 4.89; S, 2.59.

P-9. Dialdehyde **M-3** (0.5 g, 0.66 mmol) and **M-8** (0.27 g, 0.66 mmol) Yield: 0.44 g (57%) of brownish-red polymer. ^{1}H NMR (400 MHz, $CDCl_3$): δ = 8.50−6.89 (m, 20H), 4.06−3.90 (m, 8H), 1.76−0.94 (m, 60H). ^{13}C NMR (400 MHz, $CDCl_3$): δ = 160.48, 153.00, 150.29, 148.33, 145.99, 139.93, 135.02, 133,07, 131.32, 130.22, 129.94, 129.38, 127.85, 126.40, 125.45, 118.28, 117.47, 114.60, 114.34, 113.08, 70.79, 69.96, 69.66, 69.15, 39.44, 36.61, 31.71, 30.57, 29.26, 29.11, 26.08, 23.91, 22.99, 22.60, 18.68, 13.99, 11.08. GPC (THF): $\bar{M}_w$ = 14 000 g/mol, $\bar{M}_n$ = 10 500; PDI = 1.90; $\bar{P}_n$ = 9. UV−vis ($CHCl_3$): λ_{max}/nm (ϵ/(L mol^{-1} cm^{-1})): 387 (25 100), 511 (7950). Elemental analysis calculated for $(C_{74}H_{88}N_4O_4S)_n$ $(1129.58)_n$: C, 78.68; H, 7.85: N, 4.96; S, 2.84. Found: C, 77.94; H, 8.06,: N, 4.44; S, 2.45.

Supporting Information Available: Synthetic details of pre-monomers, ^{1}H NMR and ^{13}C NMR spectra of monomers, model compounds, and polymers, and CV curves of model compounds. This material is available free of charge via the Internet at http://pubs.acs.org.

References and Notes

(1) Skotheim, T. A., Elsenbaumer, R. L., Reynolds, J., Eds.; *Handbook of Conducting Polymers*, 2nd ed.; Marcel Dekker: New York, 1998.
(2) Segura, J. L. *Acta Polym.* **1998**, *49*, 319−344.
(3) Mitschke, U.; Bäuerle, P. *J. Mater. Chem.* **2000**, *10*, 1471−1507.
(4) Yu, G.; Gao, J.; Hummelen, J. C.; Wudl, F.; Heeger, A. J. *Science* **1995**, *270*, 1789−1791.
(5) Brabec, C. J.; Sariciftci, N. S.; Hummelen, J. C. *Adv. Funct. Mater.* **2001**, *11*, 15−26.
(6) Katz, H. E. *J. Mater. Chem.* **1997**, *7*, 369−376.
(7) Katz, H. E.; Bao, Z.; Gilat, S. L. *Acc. Chem. Res.* **2001**, *34*, 359−369.
(8) Wang, X.; Perzon, E.; Delgado, J. L.; de la Cruz, P.; Zhang, F.; Langa, F.; Anderson, M. R.; Inganas, O. *Appl. Phys. Lett.* **2004**, *85*, 5081.
(9) Roncali, J. *Chem. Rev.* **1997**, *97*, 173.
(10) Sariciftci, N. S.; Smilowitz, L.; Heeger, A. J.; Wudl, F. *Science* **1992**, *258*, 1474. (b) Kraabel, B.; Hummelen, J. C.; Vacar, D.; Moses, D.; Sariciftci, N. S.; Heeger, A. J. *J. Chem. Phys.* **1996**, *104*, 4267.
(11) Havinga, E. E.; ten Hoeve, W.; Wynberg, H. *Polym. Bull. (Berlin)* **1992**, *29*, 119.
(12) Havinga, E. E.; ten Hoeve, W.; Wynberg, H. *Synth. Met.* **1993**, *55*−*57*, 299.
(13) Zhang, F.; Perzon, E.; Wang, X.; Mammo, W.; Anderson, M. R.; Inganas, O. *Adv. Funct. Mater.* **2005**, *15*, 745.
(14) Wienk, M. M.; Turbiez, R.; Struijk, M. P.; Fonrodona, M.; Janssen, R. A. J. *Appl. Phys. Lett.* **2006**, *88*, 153511.
(15) Campos, L. M.; Tontcheva, A.; Günes, S.; Sonmez, G.; Neugebauer, H.; Sariciftci, N. S.; Wudl, F. *Chem. Mater.* **2005**, *17*, 4031.
(16) Wang, X.; Perzon, E.; Langa, F. F.; Admassie, S.; Anderson, M. R.; Inganas, O. *Adv. Funct. Mater.* **2005**, *15*, 1665.
(17) Thomas, K. R. J.; Lin, J. T.; Tao, Y. T.; Chuen, C. H. *Adv. Mater.* **2002**, *14*, 822.
(18) Drury, A.; Maier, S.; Rüther, M.; Blau, W. J. *J. Mater. Chem.* **2003**, *13*, 485.
(19) Egbe, D. A. M.; Kietzke, T.; Carbonnier, B.; Mühlbacher, D.; Hörhold, H. H.; Neher, D.; Pakula, T. *Macromolecules* **2004**, *37*, 8863.
(20) Miyaura, N.; Suzuki, A. *Chem. Rev.* **1995**, *95*, 2457.
(21) Egbe, D. A. M.; Bader, C.; Nowotny, J.; Günther, W.; Klemm, E. *Macromolecules* **2003**, *36*, 5459.
(22) Wagner, M.; Nuyken, O. *Macromolecules* **2003**, *36*, 6716.
(23) Apperloo, J. J.; Janssen, R. A. J.; Malenfant, P. R. L.; Frechet, J. M. J. *Macromolecules* **2000**, *33*, 7038.
(24) McBranch, D. W.; Sinclai, M. B. *The Nature of The Photoexcitations in Conjugated Polymers*; Sariciftci, N. S., Ed.; World Scientific Publishing: Singapore, 1997; Chapter 20, p 608.
(25) Rothberg, L. J.; Yan, M.; Papadimitrakopoulos, F.; Galvin, M. E.; Kwock, E. W.; Miller, T. M. *Synth. Met.* **1996**, *80*, 41.
(26) Peng, Z. *Polym. News* **2000**, *25*, 185.
(27) Ashraf, R. S.; Klemm, E. *J. Polym. Sci., Part A: Polym. Chem.* **2005**, *43*, 6445.
(28) Mühlbacher, D. Diploma thesis, Linz, Austria, 2002.
(29) Bredas, J. L.; Silbey, R.; Boudreux, D. S.; Chance, R. R. *J. Am. Chem. Soc.* **1983**, *105*, 6555.
(30) deLeeuw, D. M.; Simenon, M. M. J.; Brown, A. B.; Einerhand, R. E. F. *Synth. Met.* **1997**, *87*, 53.
(31) Liu, M. S.; Jiang, X.; Liu, S.; Herguth, P.; Jen, A. K.-Y. *Macromolecules* **2002**, *35*, 3532.
(32) Liu, Y.; Liu, M. S.; Jen, A. K.-Y. *Acta Polym.* **1999**, *50*, 105.
(33) Gerischer, H., Tobias, C. W., Eds.; *Advances in Electrochemistry and Electrochemical Engineering*; John Wiley: New York, 1977; Vol. 10, p 213.
(34) Gomer, R. J.; Tryson, G. *J. Chem. Phys.* **1977**, *66*, 4413.
(35) Kötz, R.; Neff, H.; Müller, K. *J. Electroanal. Chem.* **1986**, *215*, 331.
(36) Kitamura, C.; Tanaka, S.; Yamashita, Y. *J. Chem. Soc., Chem. Commun.* **1994**, 1585. (b) Kitamura, C.; Tanaka, S.; Yamashita, Y. *Chem. Mater.* **1996**, *8*, 570.
(37) Ashraf, R. S.; Shahid, M.; Klemm, E.; Al-Ibrahim, M.; Sensfuss, S. *Macromol. Rapid Commun.* **2006**, *27*, 1454. (b) Ashraf, R. S.; Hoppe, H.; Shahid, M.; Gobsch, G.; Sensfuss, S.; Klemm, E. *J. Polym. Sci., Part A: Polym. Chem.*, in press.
(38) Egbe, D. A. M.; Tillmann, H.; Birckner, E.; Klemm, E. *Macromol. Chem. Phys.* **2001**, *202*, 2712.
(39) Maruyama, S.; Kawanishi, Y. *J. Mater. Chem.* **2002**, *12*, 2245.
(40) Wright, M. E.; Mullick, S.; Lackritz, H. S.; Liu, L. Y. *Macromolecules* **1994**, *11*, 3009.
(41) Keegstra, M. A.; Brandsma, L. *Synthesis* **1988**, *11*, 890.
(42) Don, D. K.; Kari, A. M.; Tessa, R. C.; Melanie, R. F.; Daniel, J. S.; Seth, C. R. *J. Org. Chem.* **2002**, *67*, 9073.
(43) Park, K.; Yoshino, K.; Tomiyasu, H. *Synthesis* **1999**, *12*, 2041.
(44) Martinez-Ruiz, P.; Behnisch, B.; Schweikart, K.-H.; Hanack, M.; Lüer, L.; Oelkrug, D. *Chem.—Eur. J.* **2000**, *8*, 1294.
(45) Demas, J. N.; Crosby, G. A. *J. Phys. Chem.* **1971**, *75*, 991.

MA061231E